

## Comparative analysis for different passive filter topologies in grid-tied PV systems

Shorouk Elsayed Ibrahim Mehrez<sup>1</sup>, Asmaa Sobhy Sabik<sup>2</sup>, Fady Wadie<sup>3</sup>, Ibrahim A. Nassar<sup>4</sup>

<sup>1</sup>Department of Telecommunication Engineering, College of Engineering, Egyptian Russian University, Badr City, Egypt

<sup>2,4</sup>Department of Electrical Engineering (Electrical Power and Machines), Faculty of Engineering, Al-Azhar University, Nasr City, Egypt

<sup>3</sup>Department of Mechatronics Engineering, College of Engineering, Egyptian Russian University, Badr City, Egypt

### Article Info

#### Article history:

Received Jul 6, 2025

Revised Feb 25, 2026

Accepted Mar 4, 2026

#### Keywords:

Fast fourier transform

Grid-tied

Inductive capacitive filter

LCL filter

passive RC filter

Photovoltaic system

Total harmonic distortion

### ABSTRACT

The enhancement of power quality in grid-connected photovoltaic (PV) systems requires the development of effective harmonic mitigation techniques. This paper addresses the design and evaluation of specific passive filters (RC, LC, and LCL filters) for a three-phase grid-tied PV system, aiming to mitigate harmonics in the power system. The paper also systematically calculates and optimally solves for the components required for the given system. The design of the parameters for all filter topologies within the 100-kW grid-connected PV array is thoroughly elaborated. Each topology is evaluated based on the total harmonic distortion (THD) content, which is obtained using fast fourier transform (FFT), as well as DC voltage and system efficiency. The results are presented to identify the best solutions for harmonic mitigation. The modified filter model demonstrated in this study effectively limits harmonic distortion at the output. It is shown that the proposed design addresses the issue of harmonic distortion in grid-connected inverters for PV systems. The goal of this paper is to identify the most reliable filter for extending the system's lifespan. The results suggest that the LCL filter is superior, as the system's DC voltage remained within the rated value and the system efficiency was higher compared to the RC filter. The performance and functionality of these filters were tested using MATLAB/Simulink.

*This is an open access article under the [CC BY-SA](https://creativecommons.org/licenses/by-sa/4.0/) license.*



### Corresponding Author:

Shorouk Elsayed Ibrahim Mehrez

Department of Telecommunication Engineering, College of Engineering

Egyptian Russian University

Badr City, Egypt

Email: shoroukmehrez2017@gmail.com or shorouk-elsayed@eru.edu.eg

## 1. INTRODUCTION

The use of renewable energy technologies is on the rise globally and is now regarded as a fundamental component of contemporary energy systems. Their greater adoption, whether in the form of standalone devices or hybrid systems integrated with an electric grid, is attributed in part to their net-positive environmental impact and inexpensive maintenance. Voltage source inverters (VSIs) are an important component of these power systems, sitting between the renewable source of energy and the electrical grid [1]. This connection is achieved via a passive filter and a step-up transformer, as shown in Figure 1.

The performance of solar PV power systems is much better when integrated within the electrical grid; however, certain issues like voltage unbalance, voltage sags and swells, low power factors, as well as current and voltage harmonics persist. One of the most serious issues of solar integrated grid systems is the

power quality of the VSI and the grid, since the output of the VSI inverter does have some harmonic distortion. In order to accomplish harmonic reduction of the VSI output voltage, in this case, an LCL filter with damping resistance was incorporated. The damping resistor eliminates the resonating problem. Nonlinear loads within the modeled system also inject harmonics into the system [2]-[4]. Table 1 summarizes previous studies on passive filters for grid-connected systems and provides a comparative overview of their main characteristics.

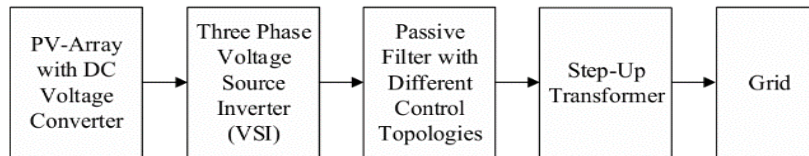


Figure 1. Block diagram of a grid connected three phase photovoltaic (PV) system

Table 1. Summary of previous studies on passive filters for grid-connected applications

Ref.	Methodology	Used system	Main outcomes	Limitations
[5]	Comparative analytical and simulation-based study of L, LC, and LCL filters	Grid-connected converter (generalized system, IEEE conference setup)	Demonstrated that LCL filters provide superior harmonic attenuation compared to L and LC filters	No experimental validation; resonance and damping issues not deeply addressed
[6]	Comprehensive review and analytical analysis of harmonic resonance phenomena	Multi-parallel grid-connected inverters	Identified harmonic resonance causes and mitigation techniques in parallel inverter systems	Review-based only; no specific filter design or optimization framework
[7]	Design and simulation-based implementation of LC and LCL passive filters	PV-based renewable energy system	LCL filter achieved lower THD and better harmonic suppression than LC filter	Increased system complexity; resonance damping not optimally addressed
[8]	Comparative simulation analysis with passive damping techniques	5-level VSC with series and parallel damped LCL filters	Parallel-damped LCL filter showed better stability and harmonic performance	Increased losses due to damping resistors; higher implementation cost
[9]	Systematic review of harmonic distortion sources and mitigation methods	Power systems with renewable energy integration	Highlighted impact of power electronics on harmonic distortion and importance of filtering	No quantitative comparison or system-level implementation
[10]	Analytical design supported by simulation results	Three-phase grid-tied PV system	Properly designed passive filters significantly improved power quality	Passive filters are bulky and less adaptive to varying grid conditions
[11]	Simulation-based design of passively damped LCL filter	Grid-connected PV system	Passive damping enhanced stability and reduced resonance effects	Reduced efficiency due to damping losses; lack of experimental results
[12]	Analytical modeling and simulation-based performance assessment	Three-phase grid-connected VSC with LCL filter	Active damping using current feedback improved system stability without additional losses	Increased control complexity and dependency on accurate sensing
Proposed study	MATLAB/Simulink-based comparative analysis of RC, LC, and LCL passive filters using FFT-based THD evaluation, DC-link voltage, and system efficiency	100-kW three-phase grid-connected PV system with inverter output filtering	The results show that the installation of passive filters is essential for harmonic mitigation. The LCL filter reduced THD to 5.66%, meeting the IEEE 519-2022 standard. It maintained the DC-link voltage close to its rated value and achieved a high efficiency of 98.2%. While RC and LC filters also reduced THD, the RC filter exhibited low efficiency, and the LC filter showed higher DC voltage deviation compared to the LCL filter.	The analysis is based solely on simulation results and does not include experimental validation

Pawar [13] outlines the modeling and simulation of the 80 kW Solar PV system connected to the grid at Shivaji University, Kolhapur, with the help of several harmonic reduction techniques employing MATLAB Simulink. The overall modeling of the Solar PV system consists of design of PV array, MPP tracking, PLL modeling, inverter control model, and LC filter, which is provided in a block schematic diagram.

The appropriate selection of a reduction technique achieves a reduction of total harmonic distortion (THD) for the power system. Pawar [13], they focus on attempting to reduce harmonic distortion from the system by passive filter techniques, especially series passive filters and combinations of shunt filters. Reducing current harmonics is most effectively achieved through the application of shunt and series passive filters combined with series capacitive reactance, as shown in this study. This statement has been proven by the second approach of this research. That is, passive shunt filters enable the reconstruction of the current spectrum induced by higher-order components of signals; thus, the current that flows into the parallel-connected filters does not contain significant harmonics and aids in improving the current quality for the consumer [14].

The remainder of the text is organized within the following framework: In section 2, there was a design of a passive filter for grid-tied PV applications, which is followed by section 3, which demonstrates the modelling and system description. Finally, the results and discussion of the simulation are presented in Section 4, followed by a conclusion in Section 5.

## 2. DESIGN OF PASSIVE FILTER FOR GRID-TIED PV-APPLICATIONS

The lowest cost solution to reduce harmonics is through passive filters which are the first choice when designing low and medium powered PV systems. However, as pointed out in the introductory section, these filters have shortcomings and still, they are widely used [10]. The RC filter is included in this study as a baseline topology due to its structural simplicity and conventional use in basic harmonic mitigation. It serves as a reference for performance comparison with more advanced LC and LCL configurations rather than as a preferred solution for high-power grid-connected application.

### 2.1. Design of RC passive filter

RC passive filters play a crucial role in the enhancement of power quality in three-phase grid-connected PV systems by filtering high-frequency harmonics. The design process of these filters requires careful attention to cutoff frequency, resistance, capacitance, damping coefficients, and component ratings. Appropriately designed RC filters allow for compliance with grid codes, system stability, and effective operation of PV systems. The purpose of using RC passive filters includes:

- Limit high-frequency harmonics that come from inverter switching.
- Boost the quality of power and maintain compliance to grid standards, i.e., IEEE 519.
- Safeguard sensitive PV system and grid components.

Design process for RC passive filters:

- Step 1: Specify system requirements.

Determine grid voltage, frequency, and harmonic standards to comply with (for instance, IEEE 519). Establish the inverter's switching frequency and its harmonic spectrum.

- Step 2: Specify cutoff frequency ( $f_c$ ).

Select a cutoff frequency that is lower than the inverter's switching frequency but much higher than the grid frequency to prevent distortion.

- Step 3: Determine component values.

Compute the relevant capacitance given the specific cutoff frequency and a selected resistance value:

$$C = 1/2\pi f_c R \quad (1)$$

- Step 4: Evaluate damping and system stability.

Commonly, in grid tied PV systems, the value of  $\xi$  is picked between (0.7 and 1) as a good choice for performance

- Step 5: Choose particular components of suitable rating.

Make sure the resistors and capacitors can manage the voltage, current, and thermal stresses generated by the system.

### 2.2. Design of LC passive filter

In a grid connected PV system, passive LC filter can be implemented to lower THD and enhance power quality improvement. This type of filtering rests on the elimination method concerning with harmonic of the network with the L-C passive elements adjustment [15]. The LC filter is simple in structure, inexpensive prices, and highly efficient as well as meets the fundamental of frequency reactance [16], [17]. The connection diagram of the LC filter is shown in Figure 2.

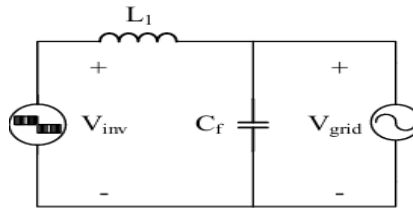


Figure 2. The connection diagram of the LC filter

To mitigate resonance issues in the LC filter, the LC filter's resonance frequency must be above ten times the fundamental frequency, but below half the switching frequency, in order to prevent resonance problems. Hence, the resonance frequency will be determined according to the limits formulated by (2):

$$10f_0 \leq f_{\text{res}} \leq \frac{f_{\text{sw}}}{2} \quad (2)$$

As  $f_0$  refers to the utility frequency, while  $f_{\text{sw}}$  is the switching frequency, and  $f_{\text{res}}$  is the corresponding resonant frequency. The resonant frequency of an LC filter situated at the jumping frequency is given by:

$$f_{\text{res}} = \frac{1}{2\pi} \sqrt{\frac{1}{LC}} \quad (3)$$

Consequently, choosing a larger capacitance value gives better attenuation of higher-order harmonic elements. But as  $C$  increases, the current flowing through  $L$  increases, thus decreasing the filter efficiency. On the contrary, a smaller  $C$  value requires a bigger  $L$ , which increases the power filter size. The reactive power of the capacitor can be expressed as follows:

$$Q_c = \frac{V_{\text{rated}}^2}{\omega C} = (2\pi f) C V_{\text{rated}}^2 \leq \alpha P \quad (4)$$

As  $Q_c$  is the reactive power taken by the capacitor with the rated voltage of the system ( $V_{\text{rated}}$ ). The reactive power absorption rate ( $\alpha$ ) is normally set less than 5%. The capacitance value ( $C$ ) depends on the specific amount of reactive power which is taken by the filter. The capacitor value should be determined by means of the equation presented in (5).

$$C = \frac{\alpha P_{\text{rated}}}{(2\pi f) V_{\text{rated}}^2} \quad (5)$$

Found as. At the fundamental frequency, the excess flow currents are restrained by a capacitor of high value. The  $L$  inductor value is obtained by ripple current calculation. The value of  $L$  is chosen according to (6).

$$L = \frac{V_{\text{dc}} - V_{\text{rated}}}{f_{\text{sw}} \Delta I} \quad (6)$$

The input voltage to the inverter is characterized by the DC voltage ( $V_{\text{dc}}$ ). The ripple current is selected from 5 to 10 percent of the rated current, and the switching frequency ( $f_{\text{sw}}$ ) is important for system performance. The inverter is filtered by means of passive LC filters, which eliminate the harmonic frequencies above the fundamental one. The proposed system is implemented and tested using the MATLAB/Simulink program [18], [19].

### 2.3. Design of LCL passive filter

Currently, many designers are giving more attention to high-order LCL filters due to their low cost and efficient results in grid-tied PV applications. Figure 3 shows the topology of a passive LCL filter with VSI integration [20]. The specifications of an LCL-filter are functionally reliant on the system's line frequency, rating of power consumption, and switching frequency [21], [22]. To prevent any resonance problems within the system, the value of the resonant frequency must not be lower than 10 times the basic frequency while staying under half the switching frequency [11], [6]. The line frequency, resonance frequency, and inverter switching frequency are expressed in radian per second as follows:  $\omega_0$ ,  $\omega_{\text{res}}$ , and  $\omega_{\text{sw}}$ , respectively. Resonance frequency can be defined in the following way, according to (7):

$$\omega_{res} = \sqrt{\frac{L1+L2}{L1 L2 C_f}} \tag{7}$$

The use of a larger capacitor will enhance the attenuation of higher-order harmonics, but it will also draw more current from the inverter-side inductor (L1). This increases reactive power demands and subsequently decreases filter efficiency. On the other hand, decreasing the capacitance value (Cf) will require an increase in the inductance value of (L1) to satisfy the high frequency components. Thus, the selection of the Cf is become a balancing act between the reactive power that the filter will consume and the required value of the inverter-side inductor (L1). In (8) depicts the law determining the value of Cf for an LCL filter in the references [23], [24].

$$C_f = \frac{Q}{2\pi f_0 V^2_{rated}} \tag{8}$$

The line output frequency is denoted by f0, whereas Q denotes the filter’s reactive power absorption and V is the rated voltage of the system. The current ripple ΔI also affects the operational value of the inverter side inductor L1 [25]. When ripple currents increase, losses associated with switching become lower and the requirement for the inductance value of filter L1 will be increased. Thus, the choice of an optimal L1 must take into consideration the switching losses and the size of the inductor. The inductance of filter L1 can be calculated according to (9).

$$L_1 = \frac{V_{inv}}{8 \Delta I f_{sw}} \tag{9}$$

The input passive filter voltage is termed as (V<sub>inv</sub>), ripple current (ΔI) is set to approximately 5% of the rated current. The inductor on the grid side correlates to the equation (L1 = α L2) where (α) is the ratio factor of inductance. For low to medium power applications, this is often true with α > 1. This indicates that L2 < L1 which helps in minimizing the risk of overrating the switches leading to improve the system’s overall efficiency. After considering L2, if it does not meet the required resonance frequency so the quantity of reactive power that was being absorbed needs to be adjusted along with Cf [26]-[28].

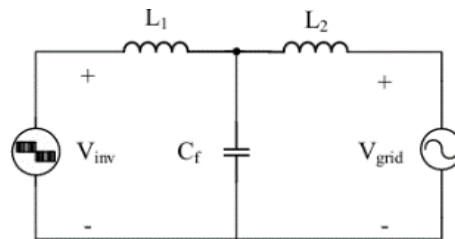


Figure 3. The topology of the passive LCL filter incorporated with VSI

**2.4. Selection criteria of passive filter components**

The equations provided above describe the mathematical design of RC, LC, and LCL filters. However, the final component values were selected based on practical engineering criteria to ensure stability, low THD, and acceptable reactive power levels.

- Capacitance (C, Cf): the capacitor was selected such that the reactive power drawn does not exceed 5% of the rated power, in accordance with common grid-code limits. This ensures that the filter does not overload the inverter or distort the grid voltage.
- Inductors: the inverter-side inductor was determined based on limiting the current ripple to 5–10% of the rated current, which guarantees low switching stress and acceptable filtering. The grid-side inductor was chosen using the ratio α=L1/L2, typically greater than 1, to ensure stability and avoid excessive voltage drop.
- Resonance frequency: all filters were designed so that the resonant frequency satisfies 10f0 < fres < 0.5fsw preventing unwanted resonance with the grid or the switching frequency.
- Damping: for RC filter, damping resistance values were chosen to avoid resonance peaks and guarantee smooth transient response.

This ensures that the selected values satisfy both theoretical design constraints and practical operation limits.

### 3. MODELLING AND SYSTEM DESCRIPTION

In this model, the 100 kW PV plant has been modeled in detail along with its connection to the 25 kV grid via a boost DC-DC converter and a three-phase three-level voltage sourced converter (VSC). The system uses a three-phase three-level VSC at the grid-side and a boost DC-DC converter for power optimization. The MPPT is done using the ‘Incremental Conductance + Integral Regulator’ method in Simulink. The detailed model contains the following components as shown in Table 2.

Table 2. Simulation parameters of the 100-kW grid-connected PV system

Parameter	Value/Type
PV plant rated power	100 kW
PV module model	SunPower SPR-305E-WHT-D
Rated power per module	305.2 W
Total number of PV modules	330
PV array configuration	66 parallel strings × 5 modules in series
Total PV array rated power	100.7 kW
Standard test conditions (STC)	1,000 W/m <sup>2</sup> , 25 °C
Number of cells per module	96
Open-circuit voltage (Voc)	64.2 V
Short-circuit current (Isc)	5.96 A
Voltage at maximum power (Vmp)	54.7 V
Current at maximum power (Imp)	5.58 A
Natural PV output voltage	273 V
DC-DC converter type	Boost converter
DC-DC converter switching frequency	5 kHz
MPPT technique	Incremental Conductance + Integral Regulator
Boosted DC-link voltage	500 V
Grid-side converter	Three-phase three-level VSC
VSC switching frequency	1,980 Hz
DC-link voltage regulation	±250 V
VSC AC output voltage	260 V
Power factor	Unity
Coupling transformer rating	100 kVA
Transformer voltage rating	260 V / 25 kV
Utility grid	25-kV distribution feeder with equivalent 120-kV transmission system
Simulation environment	MATLAB/Simulink

### 4. RESULTS AND DISCUSSION

Different categories of passive filters were applied to mitigate the harmonics and determine the PV system's effect on distribution system efficiency and dc voltage level. The 100-kW array grid-connected system with a 25-kV grid was constructed with a boost DC-DC converter and a three-phase three-level integrated VSC, as shown in Figure 4.

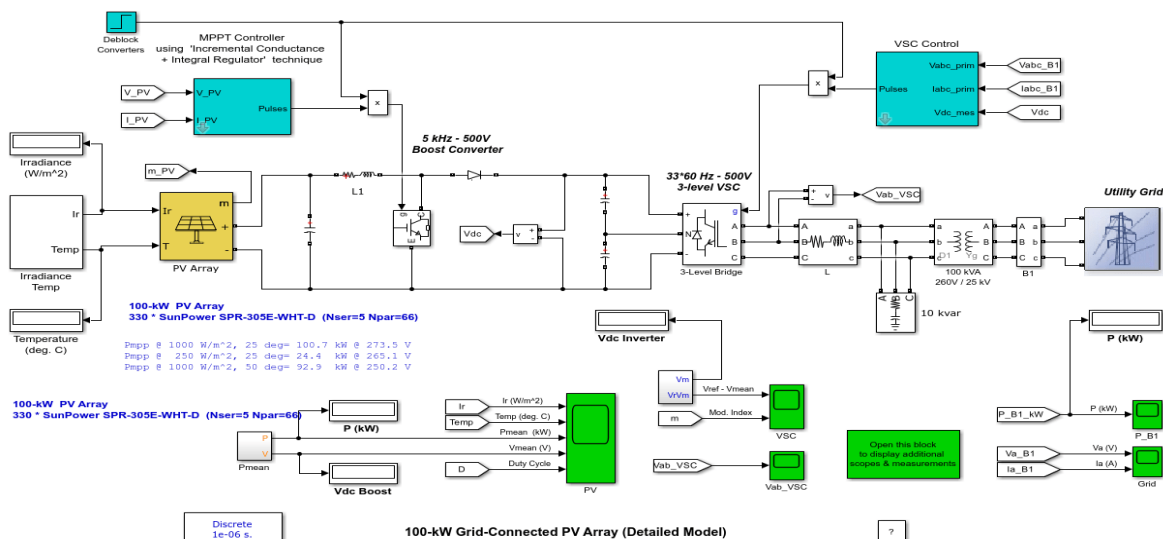


Figure 4. 100-kW grid-connected PV array (detailed model)

According to these specifications, RC, LC, and LCL passive filters are constructed with respect to parameter evaluation and their verification of results for the system done in MATLAB Simulink. The three-phase 100 KW grid tied system served as the testing system. All parameters of the topologies under consideration are presented in Table 3. Results for the system simulation with the filter and simulations of the system without filter are provided in Table 4.

Table 3. Design characteristics of different types of passive filters

	RC passive filter	LC passive filter	LCL passive filter
R(ohm)	1	---	---
L1(H)	---	2.16e-3	0.5630e-3
L2(H)	---	---	0.1407e-3
C(F)	318.31e-6	196.197e-6	196.19e-6

The results of the simulation obtained from MATLAB for the unfiltered and filtered systems are displayed below. Figure 5 shows the overall grid voltage waveforms for the unfiltered system and the system with a single-order RC filter applied. The figure illustrates how the voltage waveform and THD change when filtering is introduced. Figure 5(a) presents the grid voltage waveform without any filter applied. Figure 5(b) demonstrates THD of the unfiltered grid voltage. Figure 5(c) illustrates the grid voltage waveform after applying a single-order RC filter. Figure 5(d) indicates THD of the grid voltage after the RC filter.

**4.1. After adding a single-order RC filter**

Beginning with a single order RC-filter, the computed values of R and C were used in the filtering circuit at the output stage of the converter connected to the grid, and the THD of the grid voltage has improved to 1.26% as seen in Figure 5(d). While this single order filter has accomplished a great decline in THD, it is still not enough for grid operation. Figure 5(c) presents the waveform of the phase grid voltage after applying an RC filter, and the distortion is significantly lower than in the system without a filter. Overall, the RC filter greatly reduces THD compared to the unfiltered system, but it is still not sufficient for full compliance with grid standards, indicating the need for higher-order filters.

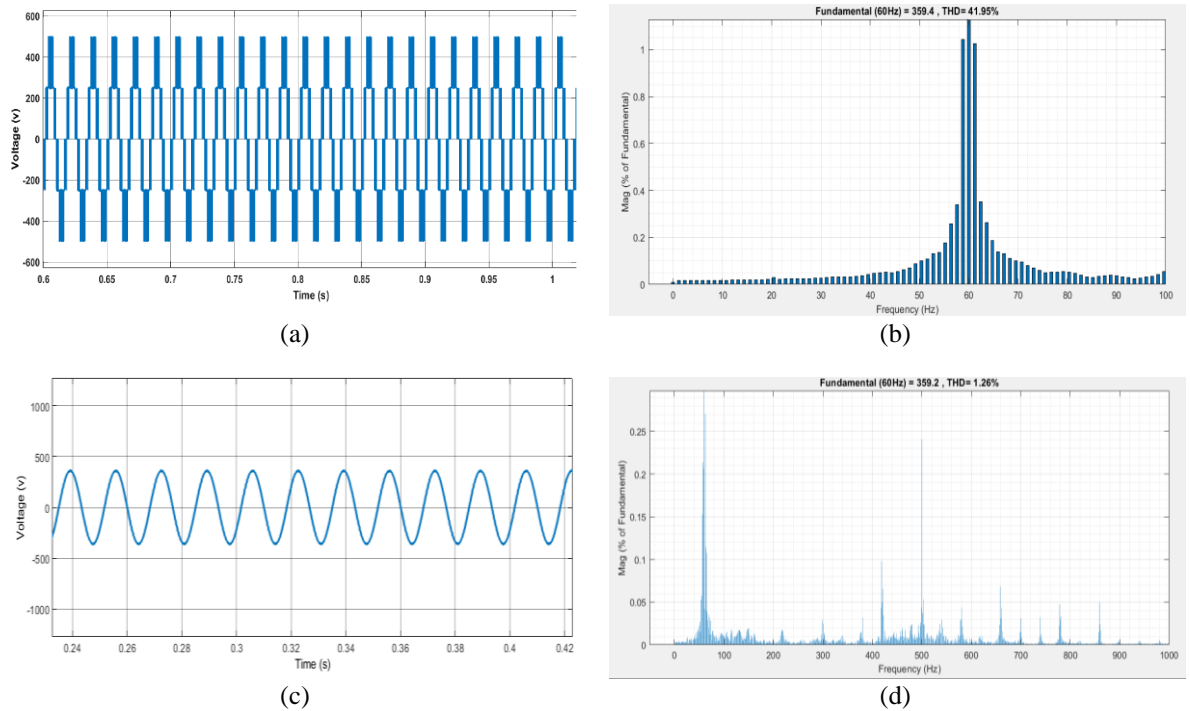


Figure 5. Simulation results without filter and using RC-filter; (a) phase voltage waveform without any filter, (b) voltage harmonic spectrum of grid connected PV system without any filter, (c) phase voltage waveform with RC filter, and (d) voltage harmonic spectrum with RC-filter

#### 4.2. After adding LC-filter

In the second-order LC filter configuration both the inductance and capacitance elements are incorporated into the filtering circuit. Where Figure 6 shows the overall grid voltage waveform when a second-order LC filter is applied at the VSC output. The figure illustrates the voltage waveform (phase voltage) and the corresponding THD under the LC filter configuration. Figure 6(a) illustrates Grid phase voltage waveform after applying the LC filter. The waveform shows a significant reduction in distortion compared to the unfiltered system. Figure 6(b) demonstrates THD of the grid voltage with the LC filter. When properly tuned to the grid system, this arrangement reduces the harmonic content of the voltage to 2.04% as shown in Figure 6(b). The implementation of the LC filter at the VSC output greatly improves the quality of current fed into the grid, but it increases the DC voltage to a higher level than the rated value. The LC filter greatly reduces the distortion on the phase grid voltage which is shown in Figure 6(a).

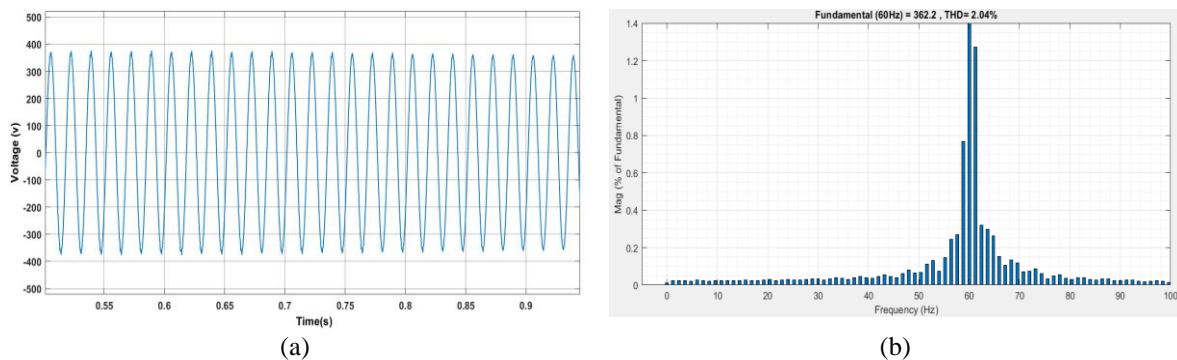


Figure 6. Simulation results of LC-filter (a) phase voltage waveform with LC filter and (b) voltage harmonic spectrum of grid-connected PV system with LC-filter

#### 4.3. After adding LCL-filter

When comparing this filter to the two filters that were previously analyzed, it is clear that this filter is considerably more effective. Where Figure 7 shows the overall grid voltage waveform when an LCL filter is applied at the VSC output. The figure illustrates both the phase voltage waveform and the corresponding THD under the LCL filter configuration. Figure 7(a) presents grid phase voltage waveform after applying the LCL filter. Figure 7(b) presents THD of the grid voltage with the LCL filter. The introduction of the LCL filter on the output side of the VSC interfacing with the grid has reduced the THD of grid voltage to about 5.66%, as it's shown in Figure 7(b). This level meets the IEEE 519-2022 standards which state that all voltage distortion on low-voltage systems at the point of common coupling (PCC) are:

- Total harmonic distortion: maximum of 8%.
- Individual harmonic components: each limited to a maximum of 5% [29].

This makes the output closely resemble sine wave which increases the system efficiency and keeps the dc voltage within the rated value. The Figure 7(a) represents the phase grid voltage waveform after applying the LCL filter and it can be seen from the figure, the distortion is very less.

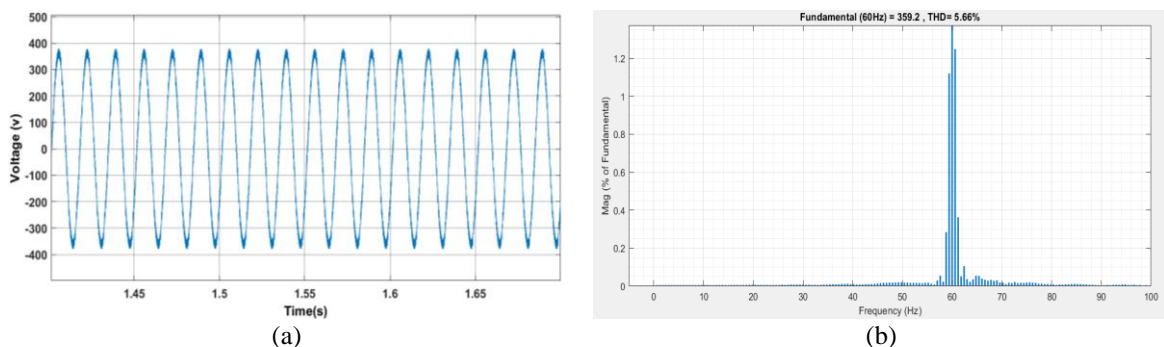


Figure 7. Simulation results of LCL-filter. (a) phase voltage waveform with LCL filter and (b) voltage harmonic spectrum of grid-tied PV system with LCL-filter

#### 4.4. Comparison between the different types of passive filters result

This subsection will focus on comparing system efficiency, dc voltage and THD before and after adding filter in all three cases, RC passive filter, LC passive filter, and LCL passive filter. From Table 4, it can be observed that dc voltage is equal to 990.77(v) for RC passive filter case at the output side of VSC connecting to grid. After LC passive filter was added to the system, dc voltage dropped to 719.27(v). Further addition of LCL passive filter to the system dc voltage had become 500.3 (v). Consequently, these indicate that the LCL filter is considerably more effective than the previous two filters. The LCL filter introduces a resonant frequency, which was properly designed and passively damped to ensure stable and reliable operation.

Table 4. Comparison between the different types of passive filters results

	RC passive filter	LC passive filter	LCL passive filter
THD before the filter (%)	41.95%	41.95%	41.95%
THD after the filter (%)	1.26%	2.04%	5.66%
Efficiency (%)	26.69%	98.68%	98.2%
Dc voltage (v)	990.77	719.27	500.3

The sensitivity of the LCL filter parameters to harmonic distortion is well-established in the literature. Increasing the inverter-side inductance  $L_1$  reduces the high-frequency current ripple injected into the grid, thereby lowering the THD. Conversely, a reduction in  $L_1$  leads to higher ripple amplitudes and consequently higher THD levels. Similarly, the filter capacitor  $C_f$  plays a central role in attenuating switching-frequency harmonics. A smaller  $C_f$  results in insufficient harmonic absorption and increased THD, whereas increasing  $C_f$  enhances harmonic suppression but may introduce excessive reactive power at the point of common coupling (PCC). These trends are consistently reported across existing studies on LCL filter design for grid-connected converters.

These findings are consistent with trends reported in previous literature, where LCL filters were highlighted for their superior harmonic attenuation capability compared to RC and LC filters. Studies such as [5]-[12] similarly confirmed that adopting an LCL structure enhances harmonic suppression while maintaining grid compliance. However, unlike some studies that focused solely on harmonic mitigation, this work additionally compared efficiency and DC voltage behavior, providing a more comprehensive evaluation.

The comparative analysis performed in this study demonstrated that the LCL filter topology provides the best overall performance among the evaluated passive filters for grid-tied PV systems. While the RC filter achieved notable THD reduction (to 1.26%), the LC filter further improved voltage quality but introduced higher DC-link voltage stress. The LCL filter achieved the optimal balance, ensuring the lowest THD, improved efficiency, and stable DC voltage level.

The findings of this study are significant because they address a critical challenge in grid-tied PV systems: maintaining power quality while minimizing harmonic distortion. Since modern grids are increasingly integrating renewable energy sources, understanding how different passive filter topologies perform under the same conditions provides engineers and researchers with practical insights for selecting the most effective filter type. The comparative results clearly demonstrate that the LCL filter achieves the lowest THD and maintains better voltage quality compared with RC and LC filters, which makes the conclusions directly relevant for designers of PV inverters, grid engineers, and researchers focused on improving the performance and reliability of distributed renewable energy systems. The efficiency is calculated as the ratio between the power delivered to the grid and the input power of the inverter. The relatively low efficiency of the RC filter is mainly due to the resistive element, which dissipates active power as heat. This inherent resistive loss increases with current magnitude, leading to reduced efficiency compared to LC and LCL topologies. Therefore, the observed efficiency values are technically justified and consistent with the filter structure.

Although the RC filter achieves the lowest THD values, its performance is associated with significant resistive power losses, resulting in reduced efficiency. In contrast, the LCL filter provides a better overall trade-off between harmonic attenuation, efficiency, and practical applicability in grid-connected PV systems. Therefore, the optimality of the filter is evaluated based on comprehensive performance criteria rather than THD alone. Although the case study is conducted on a 33-bus system, the proposed optimization framework is general and can be applied to other grid-connected PV systems. The optimal parameter values may change with network characteristics, but the methodology itself remains valid.

## 5. CONCLUSION

This work has focused on methods of harmonic mitigation and has provided the design procedure and effectiveness of passive RC, LC, and LCL filters in harmonic rejection on the output of the inverter in a PV fed system. This paper provides analysis on the THD components which its identification technique based on FFT, dc voltage, and system efficiency per each topology in order to optimize the performance of each filter. Optimized passive filter designs are critical for effective performance of grid interconnect systems. Different typologies RC, LC, and LCL are analyzed in Simulink using MATLAB for 100-kW three-phase inverter PV grid connected system. The model developed in simulation has been tested both with and without filters and it has been demonstrated that a filter should be installed for the harmonic mitigation in case the control scheme of the inverter is unable to suppress the total harmonics.

The findings of this work indicate that the dc voltage level with LCL filter is less than the voltage level with LC and RC filters when comparing these values to the rated dc voltage, and the LCL filter increases system efficiency in comparison to the RC filter. Hence, LCL filter is superior to both styles of filters discussed above. In conclusion, it is clear from the results that the LCL filter is the optimal solution as THD is reduced from 41.95% to 5.66% which is within IEEE 519-2022 standard, system efficiency improved to 98.2%, and dc voltage is at its rated value. This indicates that the third order LCL filter is more optimal than RC and LC filters. Overall, the study confirms that the LCL filter remains the most effective passive solution for harmonic mitigation in grid-connected PV systems, offering the best trade-off between power quality, efficiency, and voltage stability. These insights can support future grid-tied PV system designs aiming for improved performance and compliance with modern grid standards.

**Limitations:** while the proposed passive filter comparison demonstrates that the LCL topology provides superior performance in reducing THD and improving overall grid quality, these findings are based on simulations conducted for a 100-kW grid-tied PV system. Therefore, the optimal filter parameters might differ for systems with lower or higher capacities or for different penetration levels of distributed generation. In addition, implementing an LCL filter in real hardware may introduce practical challenges, including higher inductor costs, increased physical size, and the need for careful damping to avoid resonance. Future studies should validate these findings experimentally and evaluate the economic and physical feasibility of the filter designs across multiple PV power ratings.

**Future work:** future research may extend this work by experimentally validating the simulated results using a hardware prototype. Additional studies could investigate the impedance characteristics and resonance behavior of the filters under different grid conditions. Further optimization of LCL parameters using artificial intelligence algorithms may also be explored to enhance filter robustness and reduce switching losses. Moreover, future studies can combine the comparative analysis with optimization algorithms (such as GA, PSO, or ANN-based tuning) to automatically determine the optimal filter parameters for different grid codes.

## FUNDING INFORMATION

This research received no external funding.

## ACKNOWLEDGMENTS

The author would like to thank their supervisors for their valuable guidance and continuous support during this research work.

## AUTHOR CONTRIBUTIONS STATEMENT

This journal uses the Contributor Roles Taxonomy (CRediT) to recognize individual author contributions, reduce authorship disputes, and facilitate collaboration.

Name of Author	C	M	So	Va	Fo	I	R	D	O	E	Vi	Su	P	Fu
Shorouk Elsayed	✓	✓	✓	✓	✓	✓		✓	✓		✓		✓	
Ibrahim Mehrez														
Asmaa Sobhy Sabik	✓									✓		✓	✓	
Fady Wadie	✓											✓	✓	
Ibrahim A. Nassar												✓		

C : Conceptualization	I : Investigation	Vi : Visualization
M : Methodology	R : Resources	Su : Supervision
So : Software	D : Data Curation	P : Project administration
Va : Validation	O : Writing - Original Draft	Fu : Funding acquisition
Fo : Formal analysis	E : Writing - Review & Editing	

## CONFLICT OF INTEREST STATEMENT

Authors state no conflict of interest.

## DATA AVAILABILITY

The data that support the findings of this study are available on request from the corresponding author.




## REFERENCES

- [1] R. Pudur and M. K. Rajak, "A comprehensive review of grid-connected inverter topologies and control strategies (2020–2025)," *Next Energy*, vol. 9, p. 100433, Oct. 2025, doi: 10.1016/j.nxener.2025.100433.
- [2] M. Y. A. Khan, H. Liu, Z. Yang, and X. Yuan, "A comprehensive review on grid connected photovoltaic inverters, their modulation techniques, and control strategies," *Energies*, vol. 13, no. 6, p. 4185, Aug. 2020, doi: 10.3390/en13164185.
- [3] H. Alrajhi, S. A. Raza, H. Babsail, and A. Alattas, "Design, analysis and comprehensive assessment of LCL filters for VSC applications," *Journal of Umm Al-Qura University for Engineering and Architecture*, vol. 16, no. 3, pp. 559–573, Sep. 2025, doi: 10.1007/s43995-025-00132-1.
- [4] R. Moyal and D. Shivam, "Harmonic mitigation in modelled grid connecting solar photovoltaic array system in MATLAB," in *Proceedings of the International Conference on Industrial Engineering and Operations Management*, Aug. 2023, pp. 1246–1257, doi: 10.46254/in02.20220367.
- [5] U. P. Yagnik and M. D. Solanki, "Comparison of L, LC & LCL filter for grid connected converter," in *Proceedings - International Conference on Trends in Electronics and Informatics, ICEI 2017*, May 2017, vol. 2018-January, pp. 455–458, doi: 10.1109/ICOEI.2017.8300968.
- [6] R. Ali and T. O'Donnell, "Analysis and mitigation of harmonic resonances in multi-parallel grid-connected inverters: a review," *Energies*, vol. 15, no. 15, p. 5438, Jul. 2022, doi: 10.3390/en15155438.
- [7] M. Jayaraman and V. T. Sreedevi, "Implementation of LC and LCL passive filters for harmonic reduction in PV based renewable energy systems," in *2017 National Power Electronics Conference, NPEC 2017*, Dec. 2017, vol. 2018-January, pp. 363–369, doi: 10.1109/NPEC.2017.8310486.
- [8] I. H. Shanono, N. R. H. Abdullah, H. Daniyal, and A. Muhammad, "Performance comparison of series and parallel damped LCL filters using 5-level voltage source converter," *SN Applied Sciences*, vol. 2, no. 3, p. 471, 2020, doi: 10.1007/s42452-020-2203-8.
- [9] J. Kaur and S. K. Bath, "Harmonic distortion in power systems due to electronic control and renewable energy integration: a comprehensive review," *Discover Electronics*, vol. 2, no. 1, p. 67, Aug. 2025, doi: 10.1007/s44291-025-00111-9.
- [10] M. W. Hussain and M. A. Qureshi, "Analysis and design of passive filters for power quality improvement in 3 $\phi$  grid-tied PV systems," in *2021 4th International Conference on Energy Conservation and Efficiency, ICECE 2021 - Proceedings*, Mar. 2021, pp. 1–6, doi: 10.1109/ICECE51984.2021.9406278.
- [11] I. Chtouki, M. Zazi, M. Feddi, and M. Rayyam, "LCL filter with passive damping for PV system connected to the network," in *2016 International Renewable and Sustainable Energy Conference (IRSEC)*, Nov. 2016, pp. 692–697, doi: 10.1109/IRSEC.2016.7984020.
- [12] M. Ali, A. A. Alhussainy, F. Hariri, S. Alghamdi, and Y. A. Alturki, "Performance assessment of current feedback-based active damping techniques for three-phase grid-connected VSCs with LCL filters," *Mathematics*, vol. 13, no. 16, p. 2592, Aug. 2025, doi: 10.3390/math13162592.
- [13] P. Pawar, "Simulation and comparison of total harmonic reduction techniques of 80 kW solar Photovoltaic system at Shivaji University, Kolhapur Using Matlab Simulink," *World Journal of Engineering Research and Technology*, vol. 5, no. 4, pp. 179–195, 2019.
- [14] Y. M. Al-Sharif, G. M. Sowilam, and T. A. Kawady, "Harmonic Analysis of large grid-connected PV systems in distribution networks: a saudi case study," *International Journal of Photoenergy*, vol. 2022, pp. 1–14, Nov. 2022, doi: 10.1155/2022/8821192.
- [15] J. Lettl, J. Bauer, and L. Linhart, "Comparison of different filter types for grid connected inverter," *Progress in Electromagnetics Research Symposium*, pp. 1426–1429, 2011.
- [16] S. Adak, "Harmonics mitigation of stand-alone photovoltaic system using LC passive filter," *Journal of Electrical Engineering & Technology*, vol. 16, no. 5, pp. 2389–2396, Sep. 2021, doi: 10.1007/s42835-021-00777-7.
- [17] I. Villanueva, N. Vázquez, J. Vaquero, C. Hernández, H. López, and R. Osorio, "L vs. LCL filter for photovoltaic grid-connected inverter: a reliability study," *International Journal of Photoenergy*, vol. 2020, pp. 1–10, Jan. 2020, doi: 10.1155/2020/7872916.
- [18] Y. Zhang, C. Song, T. Wang, and K. Wang, "Optimization of passive damping for LCL-filtered AC grid-connected PV-storage integrated systems," *Electronics (Switzerland)*, vol. 14, no. 4, p. 801, Feb. 2025, doi: 10.3390/electronics14040801.
- [19] D. Kumari, "Optimal LCL filter design for grid - interfaced distributed power generation system." p. 50, 2014, [Online]. Available: <https://core.ac.uk/download/pdf/80147104.pdf>.
- [20] X. Zhou, D. Xu, and Y. Huang, "Impedance Characteristics and Harmonic Analysis of LCL-type grid-connected converter cluster," *Energies*, vol. 15, no. 10, p. 3708, May 2022, doi: 10.3390/en15103708.
- [21] M. M. Ishaya, O. R. Adegbeye, E. B. Agyekum, M. F. Elnaggar, M. M. Alrashed, and S. Kamel, "Single-tuned passive filter (STPF) for mitigating harmonics in a 3-phase power system," *Scientific Reports*, vol. 13, no. 1, p. 20754, Nov. 2023, doi: 10.1038/s41598-023-47614-7.
- [22] L. Tong, J. Deng, and X. Cao, "Numerical investigation on erosion of hydrogen stratification by steam jet within a local compartment," *International Journal of Energy Research*, vol. 44, no. 4, pp. 2665–2681, Mar. 2020, doi: 10.1002/er.5025.
- [23] G. M. Ibrahim, M. K. Ahmed, and M. I. El-Sayed, "Study of D-STATCOM impact in a grid-connected SCWEG under symmetrical fault," *Journal of Al-Azhar University Engineering Sector*, vol. 14, no. 52, pp. 926–937, 2019.




- [24] N. M. El-Naggar, M. A. Esmaeel, and S. Abu-Zaid, "Comparative performance of modular with cascaded H-bridge three level inverters," *International Journal of Electrical and Computer Engineering (IJECE)*, vol. 13, no. 4, pp. 3847–3856, Aug. 2023, doi: 10.11591/ijece.v13i4.pp3847-3856.
- [25] M. Ahmed, "On-grid photovoltaic system maximum power point tracking using perturb and observe algorithm," *Journal of Al-Azhar University Engineering Sector*, vol. 14, no. 52, pp. 1113–1122, Jul. 2019, doi: 10.21608/aej.2019.43439.
- [26] A. M. Elsherbiny, A. S. Nada, and M. Kamal, "Smooth transition from grid to standalone solar diesel mode hybrid generation system with a battery," *International Journal of Power Electronics and Drive Systems (IJPEDS)*, vol. 10, no. 4, pp. 2065–2075, Dec. 2019, doi: 10.11591/ijpeds.v10.i4.pp2065-2075.
- [27] A. A. Kandel, H. Kanaan, T. Mahmoud, and B. Saad, "Efficient reduction of power losses by allocating various DG types using the ZOA algorithm," *Results in Engineering*, vol. 23, p. 102560, Sep. 2024, doi: 10.1016/j.rineng.2024.102560.
- [28] S. Abo-Alela, "Design and performance of hybrid wind-solar energy generation system for efficiency improvement," *Journal of Al-Azhar University Engineering Sector*, vol. 13, no. 48, pp. 1118–1124, Jul. 2018, doi: 10.21608/aej.2018.18981.
- [29] IEEE Std. 519-2022, "IEEE recommended practice and requirements for harmonic control in electric power systems," *IEEE Std. 519-2022*, p. 101, 2014.

## BIOGRAPHIES OF AUTHORS






**Shorouk Elsayed Ibrahim Mehrez**    is an assistant lecturer at the Faculty of Engineering, Egyptian Russian University. She received her B.Sc. degree in Electrical Engineering from Al-Azhar University in 2018 and her M.Sc. degree from the Faculty of Engineering, Cairo University in 2023. Her research interests include renewable energy, power systems, photovoltaic systems, power quality improvement, and optimization techniques. She can be contacted at email: shoroukmehrez2017@gmail.com, shorouk-elsayed@eru.edu.eg.






**Dr. Asmaa Sobhy Sabik**    is a lecturer at Al-Azhar University, Faculty of Engineering, Electrical Engineering Department, Cairo, Egypt. She received her M.Sc. degree in Electrical Engineering (Power and Machines) in 2017 and her Ph.D. degree in Electrical Engineering in 2021 from Al-Azhar University. Her research interests include electrical machines, power systems, renewable energy technologies—particularly wind and solar energy—as well as modelling, analysis, and advanced control of energy systems. She has supervised several graduation projects and actively participates in research activities within the department. She can be contacted at email: asmaasabik2803.el@azhar.edu.eg.



**Fady Wadie**    received the B.Sc. degree in electrical power engineering in 2009 from Ain Shams University. The M.Sc. and Ph.D. degrees in high voltage engineering, from Benha university (Shoubra branch), Cairo in 2015 and 2019, respectively. He is currently a Lecturer at the Egyptian Russian University. His research activity includes switching transients of circuit breakers and their mitigation, wide area back-up protection, and fault detection algorithms based on communication assisted techniques. He can be contacted at email: enfadywadie@hotmail.com.



**Ibrahim A. Nassar**    received the B.Sc. degree in Electrical Engineering in 1999 and the M.Sc. degree in 2004 from Al-Azhar University, Cairo, Egypt. Since 2001, he has been a member of the Faculty of Engineering, Al-Azhar University. He received his Ph.D. degree from the University of Rostock, Germany, in 2011. From 2020 to 2024, he served as the Head of the Department of Electrical Engineering, Faculty of Engineering, Al-Azhar University, Cairo, Egypt. He is currently the Dean of the Faculty of Engineering (Girls' Branch), Al-Azhar University, Cairo, Egypt. He can be contacted at email: ibrahim.nassar@azhar.edu.eg.